Quantitative Analysis of Lymph Vessel Characteristics in Organ Confined Prostate Cancer

Cornelis G. van Niekerk,[1] Christina A. Hulsbergen-van de Kaa,[1]*
Jelle O. Barentsz,[2] J. Alfred Witjes,[3] and Jeroen A.W.M. van der Laak[1]

[1]Department of Pathology, Radboud University Nijmegen Medical Centre, Nijmegen, The Netherlands
[2]Department of Radiology, Radboud University Nijmegen Medical Centre, Nijmegen, The Netherlands
[3]Department of Urology, Radboud University Nijmegen Medical Centre, Nijmegen, The Netherlands

BACKGROUND. The objective of this study was to analyze the characteristics of lymphatic vasculature in normal and (peri)tumoral prostate tissue, applying accurate and objective quantification techniques based on digital image analysis.
METHODS. Radical prostatectomy specimens of 27 patients were selected containing organ confined peripheral zone tumors, which were restricted to one side of the prostate (pT2a). Lymph vessels were visualized by immunohistochemistry against D2-40. Lymphatic vessel density, perimeter, and area were assessed over the entire tumor and corresponding contralateral normal tissue. Also, morphology (area, perimeter, and diameter) of individual lymph vessels were measured in (peri)tumoral and normal tissue.
RESULTS. No differences were found in the overall lymph vasculature between tumor and normal peripheral zone. However, the area, perimeter, and diameter of individual lymph vessel profiles were significantly decreased in (peri)tumoral as compared to normal tissue. No differences were seen for these parameters between peritumoral and tumoral area. Comparing the coefficient of variation between compartments (normal, (peri)tumoral), no differences were observed for any parameter.
CONCLUSIONS. Although differences exist between the morphology of individual lymph vessels in tumor versus normal tissue, the overall vascular bed (number and summed area and perimeter of lymphatics per area unit tissue) is unaffected in tumor. Peritumoral lymphatics resemble lymphatics in tumor tissue rather than normal lymphatics. *Prostate 71: 91–97, 2011.*

KEY WORDS: **prostate cancer; lymphangiogenesis; digital image analysis**

INTRODUCTION

The in vivo visualization of prostate cancer is continuously improving as a result of new developments in imaging techniques (MRI, ultrasound) and the use of contrast agents. The contrast enhancement in these imaging modalities reflects hemodynamic changes in the prostate, providing functional rather than anatomical data. Close comparison with detailed histopathology results has contributed to a better understanding of MRI data. Signals encountered in dynamic contrast-enhanced MRI (DCE-MRI) depend on the influx and outflow of contrast agent which depends on vascular and non-vascular components. Examples are blood perfusion, microvessel density (MVD), vessel wall permeability, cell density, extracellular volume fraction, and extracellular matrix density [1]. Lymphatics are part of the vascular structure and play an important role in tissue fluid homeostasis and in transport of lymph to the central

Conflict of interest: None declared.

Grant sponsor: Dutch Cancer Foundation (KWF); Grant number: KUN 2003 2529.

*Correspondence to: Dr. Christina A. Hulsbergen-van de Kaa, MD, PhD, Department of Pathology 824, Radboud University Nijmegen Medical Centre, P.O. Box 9101, 6500 HB Nijmegen, The Netherlands.
E-mail: c.hulsbergen@pathol.umcn.nl
Received 27 January 2010; Accepted 7 June 2010
DOI 10.1002/pros.21225
Published online 14 July 2010 in Wiley Online Library (wileyonlinelibrary.com).

circulation. Insight into the characteristics of the lymph vessel vascularity of normal prostate and prostate cancer will therefore increase the understanding of contrast-enhanced radiologic imaging.

As compared to the blood vasculature, relatively limited information is available concerning the tumor lymphatic vasculature of the prostate. This can be explained by the fact that for a long time no reliable lymphatic marker has been available [2,3]. In the last 10 years several specific antibodies to lymphatic endothelial cells have been identified (human vascular endothelial growth factor receptor-3 (VEGFR-3) [4], D2-40 [5], desmoplakin [6], and LYVE-1 [7]). It was shown that the topographic distribution of lymphatic vessels in the normal human prostate shows an increased density in the capsular area, around the ejaculatory ducts and in fibromuscular regions between the transition zone (TZ) and the peripheral zone (PZ) [8,9]. In prostate cancer a significant decrease in lymphatic vessel density (LVD) was found in the intratumoral area in some studies but not in others [7,10]. In studies by Zeng et al. [10] and Roma et al. [11] an increase in peritumoral LVD was found and peritumor lymphatic invasion correlated with lymph node metastasis.

The objective of the present study was to analyze the characteristics of the overall lymph vasculature (LVD, lymphatic vessel area (LVA), and lymphatic vessel perimeter (LVP)) in tumor and peritumor tissue as compared to normal prostate tissue. Next to these commonly studied parameters describing the gross overall vasculature, digital image analysis allowed us to study the morphology (area, perimeter, and diameter) of individual lymph vessel profiles in detail. The level of accuracy reached by (semi)automated assessment may detect subtle alterations in lymph vasculature, not detected otherwise.

MATERIALS AND METHODS

Specimens

Twenty-seven (n = 27) radical prostatectomy specimens with unilateral PZ pT2 tumors were included in this study. All patients showed negative resection margins and received no neo-adjuvant therapy. The age and serum PSA levels were obtained from patient history at the time of radical prostatectomy. Prostatectomy specimens were handled according to a previously described protocol [12]. Specimens were cut into serial 4 mm transverse slices perpendicular to the dorsal rectal surface. The slices were photographed using a CCD camera. An experienced uropathologist (CHvdK) marked the borders of the tumor on hematoxylin and eosin (H&E)-stained sections. The Gleason grade and score were determined using the 2005 ISUP Modified Gleason System [13]. Tumor volume was estimated as described [14].

For this study, a mirror image of equal size compared to the tumor was marked in the contralateral normal PZ tissue to be able to obtain a measurement uninfluenced by tumoral growth factors (e.g., VEGF-C and VEGF-D) and by possible preexisting regional or zonal differences in lymph vessel parameters in the normal prostate. The peritumoral compartment was defined as the area around the tumor compartment measured within the diameter of one 10× field (i.e., 1 mm from tumor edge) containing benign glandular tissue. Mild-to-moderate chronic inflammation and various subtypes of atrophy were accepted as ''normal'' variations because of their high frequency of occurrence in prostates at the age at which adenocarcinoma occurs. Severe and extensive inflammation and multifocal high-grade PIN, however, were regarded as abnormal and excluded.

Immunohistochemistry

D2-40 immunohistochemistry was performed on sections serial to the H&E stained sections containing the marked regions of interest. A mouse anti-human D2-40 monoclonal antibody (DakoCytomation, Copenhagen, Denmark, Clone D2-40) was used as the primary antibody.

Quantification of Lymphatic Vascular Structure

Automated mapping procedure. Automated analysis of prostate specimens was performed using a method described previously [14], using KS400 image analysis software (version 3.0, Carl Zeiss, Germany). Briefly, a D2-40-stained transverse section through the entire prostate was scanned exhaustively and pseudocolor mappings were produced expressing vascular parameters assessed in local neighborhoods. Quantitative data for lymph vessel density (LVD, defined as the number of lymph vessels per unit measurement area), integrated perimeter of lymph vessels (LVP), and integrated area of lymph vessels (LVA) were extracted from scanned specimens in manually delineated regions comprising the tumor and contralateral normal tissue.

Interactive measurement. To be able to study the morphology of individual lymph vessels in more detail, in each specimen five manually selected microscopic regions were analyzed in the tumor, peritumoral, and normal area using a previously described procedure [15]. Because of the limited number of lymphatic vessels present in the prostate, fields containing multiple lymph vessels were selectively sampled if available. Images

(measuring 0.73 mm^2) were acquired using an RGB-CCD camera (DXC-950P, Sony) connected to an Axiophot microscope (Carl Zeiss) using a 10× objective (Plan Neofluar, NA = 0.3), resulting in a specimen level pixel size of $1.28 \times 1.28\,\mu m^2$. All image acquisition and processing were performed using KS400 image analysis software (version 3.0, Carl Zeiss). Positively stained vascular profiles were automatically recognized, results were shown on the computer monitor and interactive correction was performed if required. Subsequently, the software calculated the perimeter, area, and diameter of all individual vascular profiles in a field of vision.

Statistical Analysis

The skewed distribution observed for most parameters could be transformed to an approximately normal distribution using log conversion (data not shown). Comparison of data from different regions (peritumoral, tumoral, and normal tissue) was performed using either paired *t*-tests (two regions) and repeated measures analysis of variance (ANOVA) with Sidak correction of *P*-values in multiple comparison testing. The relationship of vessel parameters with tumor volume, PSA, and Gleason score was analyzed using Pearson correlation coefficients. All statistics were performed using SPSS software (SPSS, Inc., Chicago, IL). All probabilities from statistical tests are based on two-sided testing, significance being defined as $P < 0.05$.

RESULTS

Mean patient age was 60.4 years (range 47–70 years) with mean preoperative PSA of 6.43 ng/ml (range: 2.33–12.1 ng/ml). Tumors were generally small with a volume ranging from 0.3 to 4.8 cm^3 (mean 1.56 cm^3). The Gleason grade ranged from 2 to 5 (mean 3.33) with mean Gleason score 6.5 (range 5–9; Table I).

TABLE I. Clinicopathological Data of 27 Adenocarcinomas of the Prostate

Patient parameters	Number of patients (%)
Age (years)	
<60	10 (37)
≥60	17 (63)
Tumor volume (cm^3)	
≤0.5	3 (11)
0.5–3	20 (74)
≥3	4 (15)
Gleason score	
<7	15 (56)
≥7	12 (44)
PSA (ng/ml)	
<10	25 (93)
≥10	2 (7)

D2-40 immunohistochemistry resulted in a clearly visible brown sediment on lymphatics (Fig. 1). The automated pseudocolor mappings provided an overview of the spatial distribution of the lymphatic vasculature, clearly showing the limited amount of lymphatics (see example in Fig. 2). No clear spatial organization could be detected in the lymphatics layout; rather they were randomly distributed throughout the prostate. This is reflected in the fact that no significant differences existed between normal tissue and tumor tissue for any of the vessel parameters (LVD, LVA, and LVP) assessed using automated mapping (Table II). Heterogeneity of lymph vasculature between tumor and normal lymph vessels, as expressed in the coefficient of variation (CV, defined as the ratio

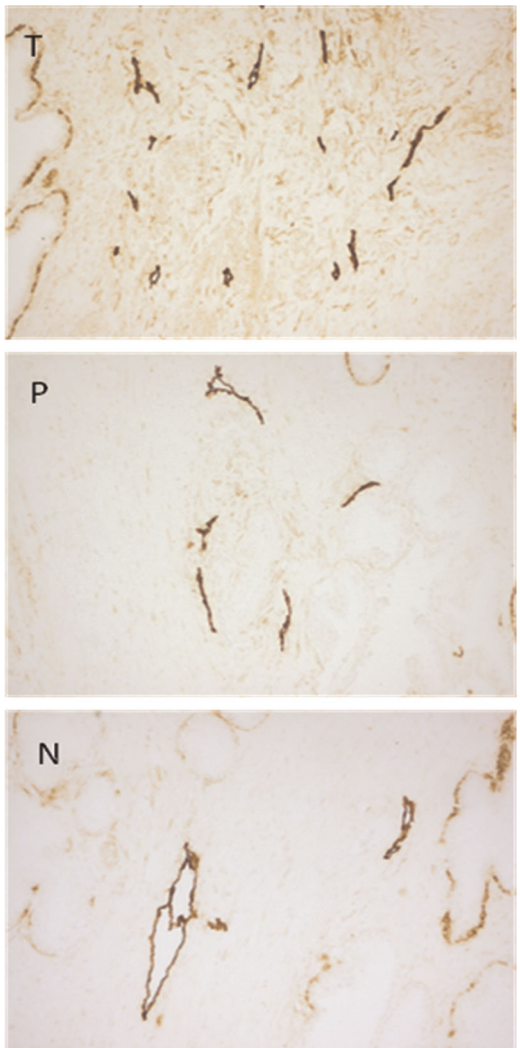

Fig. 1. Examples of immunohistologically stained (mAb D2-40) prostate tissue, showing strongly positive lymphatic vessels. Small or collapsed lymphatics were frequently found in both the tumor (T) and peritumoral (P) tissues. In normal (N) tissue the lymph vessels appeared dilated.

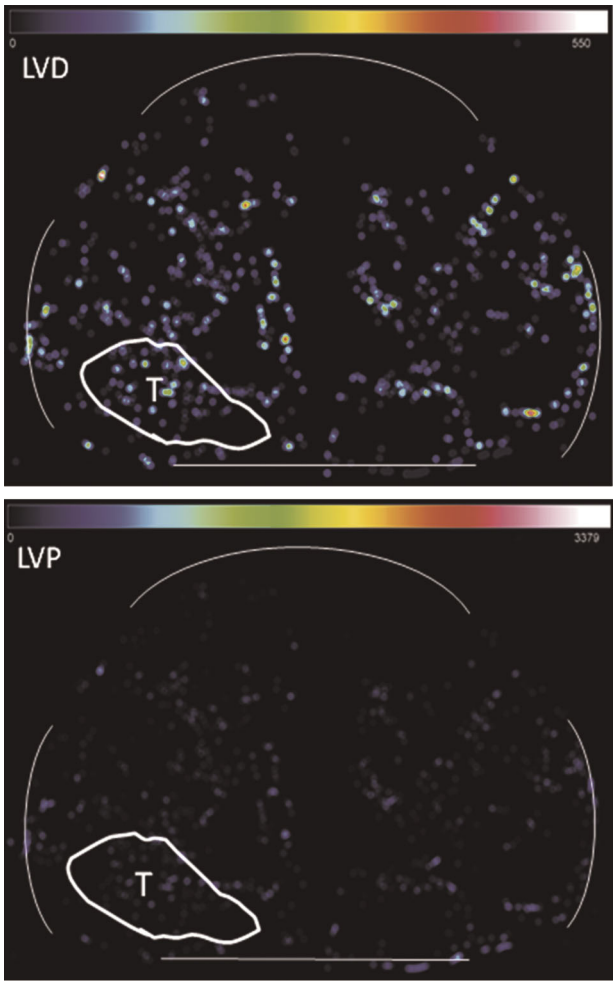

Fig. 2. Automated mapping images, illustrating lymph vessel density (LVD) and lymph vessel perimeter (LVP). LVD and LVP are shown as pseudocolors, with the corresponding scale shown on top. White lines demarcate the borders of the mapping and of the tumor (T, tumor) measured.

between standard deviation and mean value) also did not show any differences (Table II).

Figure 3 shows the (log converted) ratio between parameters assessed in different compartments. A value of 0 indicates a parameter was identical in two compartments, whereas values exceeding 0 indicate an increase in the first compartment and vice versa. Figure 3 shows a comparison of lymphatic parameters measured in tumor versus contralateral normal tissue using interactive and automated mapping measurements with each circle representing a single case (N = 27). Both the mean value and CV for lymphatic parameters assessed by the automated method cluster around 0, indicating identical parameter values in these two compartments.

Results of the interactive measurement method are shown in Table III. Highly statistical significant differences were observed for mean lymph vessel area, perimeter and diameter in normal versus peritumoral and normal versus tumor tissue (Table IV). In contrast, vessel characteristics only showed minor differences comparing peritumoral versus tumor lymphatics. The CV only proved significant for diameter in normal versus tumor tissue ($P < 0.01$). Figures 3 and 4 graphically show these data.

No relation was found between measured lymph vessel characteristics and age, tumor volume, Gleason score, and PSA (data not shown).

DISCUSSION

The complex dynamics of (blood, lymph) fluid transport through human tissues, and alterations therein caused by malignant processes form the basis of success of DCE-MRI. Understanding these dynamics will consequently aid the interpretation of DCE-MRI

TABLE II. Summary Statistics and Statistical Test Results for Mapping Data

		Normal tissue		Tumor tissue		
Parameter	Statistic	Mean	Std. dev	Mean	Std. dev	t-Test (normal vs. tumor)
LVD ($1/mm^2$)	Mean	10.6	2.48	10.7	2.16	ns
	P75	16.9	3.16	16.5	3.0	ns
	CV	73.4	10.9	71.9	9.1	ns
LVA (%)	Mean	1.1	0.7	1.0	0.5	ns
	P75	1.4	0.9	1.2	0.65	ns
	CV	147.5	33.2	153.9	34.2	ns
LVP (mm/mm^2)	Mean	1.5	0.4	1.39	0.3	ns
	P75	2.17	0.5	2	0.4	ns
	CV	91.2	12.1	91.1	10.5	ns

P75, 75th percentile; CV, coefficient of variation.
Paired *t*-tests performed on log-transformed data.
Lymph vessel density (LVD), lymph vessel area (LVA), and lymph vessel perimeter (LVP) do not show any significant differences between normal and tumor tissues.

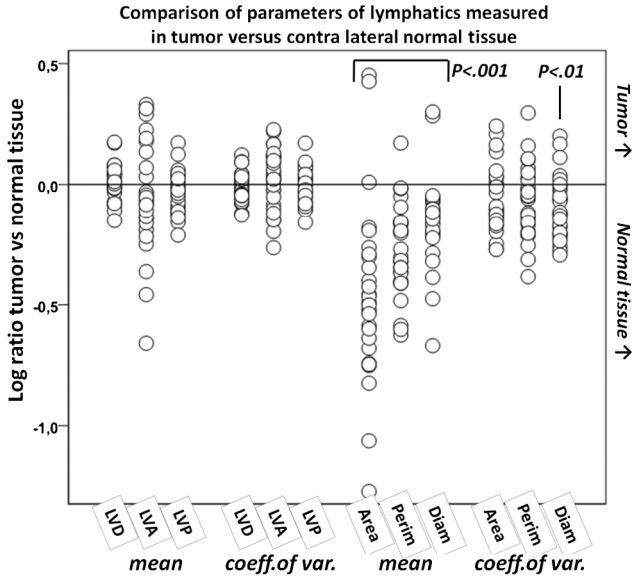

Fig. 3. Comparison of parameters of lymphatics measured in tumor versus contralateral normal tissue. Each circle represents a single case. A value of zero means no difference exists between tumor and normal tissue; positive values indicate an increased value in tumor and negative values indicate increased value for normal tissue. Measurements were performed with the automated mapping procedure (n = 27; LVD, lymph vessel density; LVA, lymph vessel area; LVP, lymph vessel perimeter) and interactively (n = 27).

signals, and may elucidate why certain tumors are more easily detected than others. In a previous study we focused on the microvascular bed in PZ prostate tumors [14]. In the present study the lymphatic bed was analyzed in such tumors, because lymphatics are also an important factor related to tissue fluid dynamics. The lymphatic bed may in this context be regarded as complementary to the microvasculature. Contradictory to most other studies, in the present study no differences were found between tumor and normal tissue regarding the extent of the lymphatic bed as expressed in the lymph vessel density (LVD). In addition to the gross overall lymphatic density, we also assessed the geometry of individual lymph vessel profiles. Significantly smaller (area, perimeter, and diameter) profiles were observed intratumorally and in the tumor periphery as compared to normal prostate. The degree of variation in these parameters was identical in all compartments.

Although previous studies agree on the intratumoral LVD being significantly smaller than the peritumoral LVD, inconsistent results were found concerning normal prostate tissue. Normal prostate was found to possess increased [7,11,16], similar [10], or even decreased [17] LVD compared to tumor tissue. Differences between such findings may often be attributed to variations in methodology [15]. In these studies, microscopic areas for assessment of LVD were selected using a variety of techniques: exhaustive sampling [11], random sampling [10], and identification of one [16] or several [7,17] subjective hot spots. Also, the group of patients investigated ranged from containing 64% low grade (Gleason grade <7) [17] to only 9% low-grade tumors [7]. Expectedly, these variations will influence study outcome.

In the present study, an objective procedure for the assessment of LVD and related parameters LVP and LVA was used [14]. Because transverse sections through the entire prostate were measured, parameters were assessed in the entire tumor as well as in the most representative (contralateral) normal tissue. This method differs from previously published studies, in which only a ''representative'' part of tumors was measured. Selection of the tumor part to be analyzed introduces undesirable bias to these studies. Also, by measuring normal tissue distant from the tumor, the influence of tumor secreted factors (e.g., VEGF) on the LVD was kept to a minimum in the present study. All other studies define normal tissue as tissue at a distance exceeding 1 mm (in one case 2 mm [16]) from the tumor edge. It is questionable whether this tissue close to the tumor may be regarded as entirely normal. Moreover, the degree in which such normal tissue is influenced by

TABLE III. Summary Statistics for Interactive Measurement Data

		Normal tissue		Peritumoral tissue		Tumor tissue	
Parameter	Statistic	Mean	Std. dev	Mean	Std. dev	Mean	Std. dev
Area (μm^2)	Mean	2,647	2,039	1,207	786.6	980.7	970.8
	CV	1.7	0.6	1.6	0.6	1.4	0.4
Perimeter (μm)	Mean	272	94.7	183.9	66	144.4	47.48
	CV	1.1	0.2	0.9	0.3	0.9	0.2
Diameter (μm)	Mean	20.91	9.25	16.05	5.7	14.98	7.95
	CV	0.9	0.3	0.8	0.2	0.7	0.2

A comparison of lymph vessel morphology (area, perimeter, and diameter) with normal, peritumoral, and tumor tissue.

TABLE IV. Statistical Test Results for Interactive Measurement Data

Parameter	Statistic	N vs. P	P vs. T	N vs. T
Area	Mean	$P < 0.001$	ns	$P < 0.001$
	CV	ns	ns	ns
Perimeter	Mean	$P < 0.001$	$P < 0.01$	$P < 0.001$
	CV	ns	ns	ns
Diameter	Mean	$P < 0.01$	ns	$P < 0.001$
	CV	ns	ns	$P < 0.01$

Tests performed using repeated measures ANOVA on log-transformed data. Sidak correction for *P*-values was used in multiple comparisons. The morphological parameters area, perimeter, and diameter show significant decrease in (peri)tumoral tissue compared to normal tissue. Lymph vessel characteristics in tumor tissue were not different from those in peritumoral tissue. Variability in lymph vessel parameters (expressed in the CV) were mostly constant over all tissue compartments.

the tumor may depend on tumor characteristics (e.g., Gleason score).

No previous studies quantitatively assessed geometry of individual lymph vessels. However, it was described that lymph vessels are either small and collapsed or large with open lumina in normal prostate [10,17]. In contrast, the presence of only small collapsed vessels in tumor tissue was observed [10,17]. These observations match our observation of tumor lymphatics being smaller compared to normal tissue. Interestingly, Kim found mainly large lymphatics in the peritumoral region whereas Zeng describes small, collapsed vessels in this region. In the present study peritumoral lymph vessels seem to resemble tumor lymphatics rather than normal lymphatics, matching Zengs' observation.

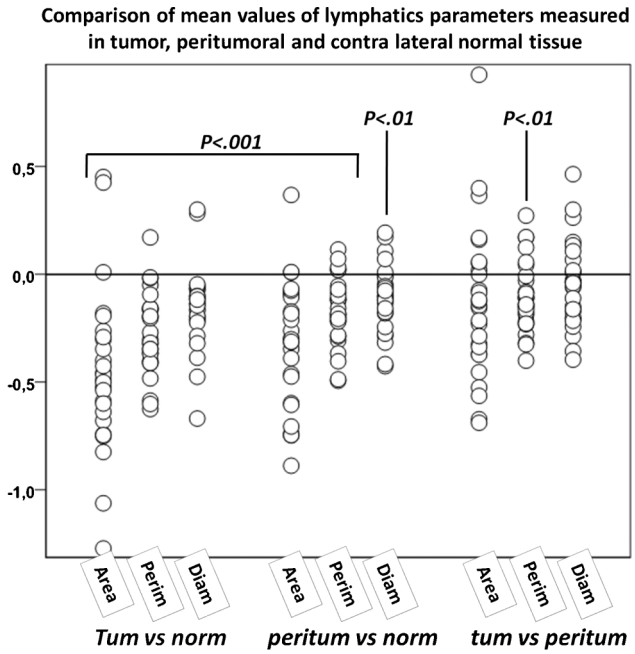

Fig. 4. Comparison of mean values of lymphatic parameters measured in tumor, peritumoral, and contralateral normal tissue. Each circle represents a single case. See legend of Figure 4 for explanation of the *y*-scale used.

From these results, we hypothesize that overall there is no difference in LVD between tumor and normal tissue. Results from previous studies may be influenced by selection criteria for normal and tumor tissue, and by criteria for selecting measurement regions within these compartments. A growing tumor mass is obliged to induce lymph angiogenesis to remain at the same overall LVD, as observed in the present study. Our results seem to indicate a limited amount of lymphangiogenesis. This is supported by the fact that prostate tumors show upregulation of VEGF-C [18]. The fact that in the present study intratumoral and peritumoral lymphatics were significantly smaller compared to normal lymphatics supports this view. Because no large-scale lymph angiogenesis takes place, differences in the morphology of individual lymphatics were not sufficiently reflected in the parameters LVA and LVP to reach significance in the present study. We therefore disagree with Trojan who argued that destruction of lymphatics takes place within prostate tumors [7].

The results of this study indicate that contrast enhancement and late washout of Gadolinium in DCE-MRI are not caused by alterations in the number of tumor lymphatics. In contrast, in a previous study we showed that increased numbers of blood vessels may be an important factor [14]. Diminished drainage due to smaller and less functional lymphatic capillaries may still have a significant impact on DCE-MRI signals.

CONCLUSIONS

By applying accurate and objective computerized measurement techniques, we were able to study both characteristics of the overall lymphatics and of individual lymphatic profiles, in tumor, peritumor, and representative normal prostate. Our results are suggestive for a limited degree of lymphangiogenesis in low-grade PZ prostate cancer.

REFERENCES

1. Tofts PS. Modeling tracer kinetics in dynamic Gd-DTPA MR imaging. J Magn Reson Imaging 1997;7:91–101.
2. Straume O, Jackson DG, Akslen LA. Independent prognostic impact of lymphatic vessel density and presence of low-grade lymphangiogenesis in cutaneous melanoma. Clin Cancer Res 2003;9:250–256.

3. Valencak J, Heere-Ress E, Kopp T, Schoppmann SF, Kittler H, Pehamberger H. Selective immunohistochemical staining shows significant prognostic influence of lymphatic and blood vessels in patients with malignant melanoma. Eur J Cancer 2004;40:358–364.
4. Jussila L, Valtola R, Partanen TA, Salven P, Heikkila P, Matikainen MT, Renkonen R, Kaipainen A, Detmar M, Tschachler E, Alitalo R, Alitalo K. Lymphatic endothelium and Kaposi's sarcoma spindle cells detected by antibodies against the vascular endothelial growth factor receptor-3. Cancer Res 1998;58:1599–1604.
5. Kahn HJ, Marks A. A new monoclonal antibody, D2-40, for detection of lymphatic invasion in primary tumors. Lab Invest 2002;82:1255–1257.
6. Ebata N, Nodasaka Y, Sawa Y, Yamaoka Y, Makino S, Totsuka Y, Yoshida S. Desmoplakin as a specific marker of lymphatic vessels. Microvasc Res 2001;61:40–48.
7. Trojan L, Michel MS, Rensch F, Jackson DG, Alken P, Grobholz R. Lymph and blood vessel architecture in benign and malignant prostatic tissue: Lack of lymphangiogenesis in prostate carcinoma assessed with novel lymphatic marker lymphatic vessel endothelial hyaluronan receptor (LYVE-1). J Urol 2004;172:103–107.
8. Soh S, Ishii T, Sato E, Akishima Y, Ito K, Baba S. Topographic distribution of lymphatic vessels in the normal human prostate. Prostate 2005;63:330–335.
9. Fukuda H, Yamada T, Kamata S, Saitoh H. Anatomic distribution of intraprostatic lymphatics: Implications for the lymphatic spread of prostate cancer—A preliminary study. Prostate 2000; 44:322–327.
10. Zeng Y, Opeskin K, Horvath LG, Sutherland RL, Williams ED. Lymphatic vessel density and lymph node metastasis in prostate cancer. Prostate 2005;65:222–230.
11. Roma AA, Magi-Galluzzi C, Kral MA, Jin TT, Klein EA, Zhou M. Peritumoral lymphatic invasion is associated with regional lymph node metastases in prostate adenocarcinoma. Mod Pathol 2006;19:392–398.
12. van Oort IM, Bruins HM, Kiemeney LA, Knipscheer BC, Witjes JA, Hulsbergen-van de Kaa CA. The length of positive surgical margins correlates with biochemical recurrence after radical prostatectomy. Histopathol 2010;56:464–471.
13. Epstein JI, Allsbrook WC, Amin MB, Egevad LL. The 2005 International Society of Urological Pathology (ISUP) Consensus Conference on Gleason Grading of Prostatic Carcinoma. Am J Surg Pathol 2005;29:1228–1242.
14. van Niekerk CG, van der Laak JAWM, Borger ME, Huisman HJ, Witjes JA, Barentsz JO, Hulsbergen-van de Kaa CA. Computerized whole slide quantification shows increased microvascular density in pT2 prostate cancer as compared to normal prostate tissue. Prostate 2009;69:62–69.
15. Vlems F, van der Worp E, van der Laak JAWM, van de Velde C, Nagtegaal I, van Krieken JHJM. A study into methodology and application of quantification of tumour vasculature in rectal cancer. Virchows Arch 2004;445:263–270.
16. Cheng L, Bishop E, Zhou H, Maclennan GT, Lopez-Beltran A, Zhang S, Badve S, Baldridge LA, Montironi R. Lymphatic vessel density in radical prostatectomy specimens. Hum Pathol 2008; 39:610–615.
17. Kim HS, Sung W, Lee S, Chang SG, Park YK. Lymphatic vessel densities of lymph node-negative prostate adenocarcinoma in Korea. Pathol Res Pract 2009;205:249–254.
18. Trojan L, Rensch F, Voss M, Grobholz R, Weiss C, Jackson DG, Alken P, Michel MS. The role of the lymphatic system and its specific growth factor, vascular endothelial growth factor C, for lymphogenic metastasis in prostate cancer. BJU Int 2006;98:903–906.